Weed Science, 53:242–251. 2005

Symposium

A review of remote sensing of invasive weeds and example of the early detection of spotted knapweed (*Centaurea maculosa*) and babysbreath (*Gypsophila paniculata*) with a hyperspectral sensor

Lawrence W. Lass
Corresponding author. Department of Plant, Soil, and Entomological Sciences, University of Idaho, Moscow, ID 83844-2339; llass@uidaho.edu

Timothy S. Prather
Department of Plant, Soil, and Entomological Sciences, University of Idaho, Moscow, ID 83844-2339

Nancy F. Glenn
Department of Geosciences, Idaho State University-Boise Center, Boise, ID 83713

Keith T. Weber
GIS Training and Research Center, Idaho State University, Pocatello, ID, 83209-8130

Jacob T. Mundt
Department of Geosciences, Idaho State University-Boise Center, Boise, ID 83713

Jeffery Pettingill
Bonneville County Weed Department, Idaho Falls, ID 83402

Remote sensing technology is a tool for detecting invasive species affecting forest, rangeland, and pasture environments. This article provides a review of the technology, and algorithms used to process remotely sensed data when detecting weeds and a working example of the detection of spotted knapweed and babysbreath with a hyperspectral sensor. Spotted knapweed and babysbreath frequently invade semiarid rangeland and irrigated pastures of the western United States. Ground surveys to identify the extent of invasive species infestations should be more efficient with the use of classified images from remotely sensed data because dispersal of an invasive plant may have occurred before the discovery or treatment of an infestation. Remote sensing data were classified to determine if infestations of spotted knapweed and babysbreath were detectable in Swan Valley near Idaho Falls, ID. Hyperspectral images at 2-m spatial resolution and 400- to 953-nm spectral resolution with 12-nm increments were used to identify locations of spotted knapweed and babysbreath. Images were classified using the spectral angle mapper (SAM) algorithm at 1, 2, 3, 4, 5, and 10° angles. Ground validation of the classified images established that 57% of known spotted knapweed infestations and 97% of known babysbreath infestations were identified through the use of hyperspectral imagery and the SAM algorithm.

Nomenclature: Babysbreath, *Gypsophila paniculata* L. GYPPA; spotted knapweed, *Centaurea maculosa* Lam. CENMA.

Key words: Hyperspectral sensor, imaging spectrometer, invasive plant detection.

Early detection of invasive plants when their spatial extent is small reduces the cost of control and increases the possibility of successful eradication (Rejmánek and Pitcairn 2002). Classifying images from remotely sensed data enhances detection of infestations. Detection abilities have improved because sensor technology and classification techniques have become more sophisticated.

Remote sensing technology has been used to detect many different invading species found in forest, rangeland, and pasture environments. This article provides a comprehensive review of the technology and algorithms used to process data for remote sensing weeds in pasture and range and a working example of the detection of spotted knapweed (*Centaurea maculosa* Lam. Syn. *C. biebersteinii* DC. or *C. stoebe* L. subsp. microanthos (Gugler) Hayek) and babysbreath (*Gypsophila paniculata* L.).

Technology

Early work on detection of weeds in rangeland and pastures with aerial photographs was generally limited to small areas because of the high cost of near-infrared image acquisitions and photo interpretation (Arnold et al. 1985). Aerial photographs work best for weed detection when plants have unique growth patterns different from surrounding vegetation (Everitt et al. 1996). Aerial photographs were found to be useful to detect saltcedar (*Tamarix ramosissima* Ledeb.) (Everitt et al. 1996), leafy spurge (*Euphorbia esula* L.) (Anderson et al. 1996), and Brazilian pepper (*Schinus terebinthifolius* Raddi) (Bellmund and Kitchens 1997; Pearlstine et al. 1998). Aerial photography has not been widely used for weed detection in rangeland and pastures because of the absence of quantitative data, high cost of color-infrared film and processing, variable interpretation, and the requirement for manual scanning or digitizing to use information in a geographic information system (GIS) (Arnold et al. 1985). Recent technological advances in digital aerial photography have improved the spatial resolution, and the color images are being used again for weed detection in limited areas. Cameras are small and light enough to attach to various aircraft, e.g., kites (Haefner 2004), balloons (Lindholm 2004), and ultralite or unmanned aircraft (RotoKraft 2004). Complications from image rectification and coregistration with ground coordinates continues to limit the use to the more expensive systems that integrate pitch, roll, and yaw measurements with global positioning system (GPS) data to determine location when imaging large areas.

Multispectral remote sensing improves on aerial photography by recording the intensity of reflected light at several different spectral wavelengths in the electromagnetic spectrum. In 1972, the first satellite to offer continuous coverage of the earth surface with multispectral data was the National Aeronautics and Space Administration (NASA) Landsat multispectral scanner system (MSS). MSS image data provided green (500 to 600 nm), red (600 to 700 and 700 to 800 nm), and near-infrared (800 to 1,100 nm) reflectance data. The spatial resolution was about 80 by 80 m with an 18-d revisit cycle. MSS data was inexpensive (then about $2,000 per 185- by 170-km image scene, and historic data can be now purchased at about $200[1,2]); however, the low spatial resolution prohibited most weed detection. Several researchers found that vegetation could be grouped into different habitat classes, including weeds (Prather et al. 1994; Ringrose and Matheson 1987). MSS data collection stopped in 1992 but continues to be useful in predicting where specific weeds may be found or likely to spread on the basis of the vegetation type and changes in vegetation.

Landsat Thematic Mapper (TM) was introduced in 1982 and provided seven spectral bands (blue to infrared) including a thermal band. The spatial resolution was 30 by 30 m in the visible and near infrared bands (bands 1 to 5 and 7) but the thermal band (band 6) had a spatial resolution of 120 by 120 m. A TM data scene was about the same size as an MSS scene, and the associated costs were about $4,000 per scene in the late 1990s (currently one TM scene costs approximately $425).[3] The higher spatial and spectral resolution allowed the detection of weeds forming large dense patches about 0.5 ha in size (Anderson et al. 1992, 1993; Everitt and Deloach 1990; Everitt et al. 1992; USGS 2003). Enhanced Thematic Mapper Plus (ETM+) replaced TM as part of Landsat 7. ETM+ had the same spectral bands as Landsat TM, but the thermal band has 60-m spatial resolution and the new panchromatic band is 15 m. A scan line corrector failure occurred in May 2003, and since then ETM+ has been impaired. Data are still available, and the pricing has been reduced from $600 to $250[4] per scene because of data gaps from the failure.

In 2000, NASA launched an additional satellite, the Earth Observing-1 (EO-1) satellite. The EO-1 satellite has three sensors on board and two pertain to weed detection: Advanced Land Imager (ALI) with 10 bands including a panchromatic band with 10-m spatial resolution and a thermal band with 30-m spatial resolution, and Hyperion, a 220-band hyperspectral sensor (357 to 2,576 nm in 10-nm bandwidth increments) with 30-m spatial resolution. The scene width for the ALI is 37 km and for the Hyperion it is 7.7 km. The standard scene length is 42 km and is targeted to user-specified areas. The cost per scene is about $1,500 for requesting a site and $250 for archive data.[5] ALI and Hyperion data have been used to detect leafy spurge (Root 2002).

Other satellite platforms also have been used to detect weeds in terrestrial environments. The Advanced Very High Resolution Radiometer (AVHRR)[6] instrument (commonly called the weather satellite) has a 1,100-m spatial resolution at nadir (straight down). These images are ideal for weed species forming large dense patches and have been used to detect broom snakeweed [*Gutierrezia sarothrae* (Pursh) Britt & Rusby] (Peters et al. 1992). AVHRR data are obtained continuously with both morning and afternoon collections and are available at no cost to the public (http://edc.usgs.gov/products/satellite/avhrr.html).

The French satellite system SPOT,[7] with 20-m multispectral data (green from 500 to 590 nm, red from 600 to 680 nm, and near-infrared from 790 to 890 nm), recently improved its spatial resolution to 5 m color data and 2.5 m panchromatic (510 to 700 nm). New, high spatial resolution data are available from commercial satellites such as Quickbird and Ikonos. Quickbird's multispectral bands have 2.4-m spatial resolution, whereas the panchromatic band has 0.6-m spatial resolution. Quickbird records blue reflectance from 450 to 520 nm, green from 500 to 520 nm, red from 630 to 690 nm, and near infrared from 760 to 900 nm. The instrument recorded a panchromatic band that ranges from 450 to 900 nm. The spatial resolution for Ikonos is 4 m multispectral and 1 m panchromatic. The spectral bands on Ikonos range from 450 to 520 nm for blue, 510 to 600 nm for green, 630 to 700 nm for red, and 760 to 850 nm for near infrared. The Ikonos panchromatic band ranges from 450 to 900 nm. The spatial resolution may be improved using the panchromatic band to sharpen the imagery to about 1 m. The costs of Ikonos and Quickbird data are about $20,000 for a 20- by 40-km image area for four bands plus panchromatic, but archive data (older than 6 mo) may be purchased for about $8,000.[8]

Higher spatial resolution than what are available with current satellite systems is often required to detect weed infestations. Older satellite systems with 20-, 30-, and 80-m spatial resolution imagery could not detect small infestations or weeds mixed with other vegetation. The satellite data were often not available during peak bloom or other detectable phenological stages. Commercial remote sensing companies using digital video and still cameras with spectral filters have found a marketing niche when satellite data are not available or useful for detecting weeds in rangeland and forest. Multispectral airborne imaging systems provide spatial resolution ranging from 0.25 to 4 m depending on the height of the instrument and contain three to eight cameras. Each camera has the capability to record light in 10- to 70-nm bandwidths ranging from 400 to 1,200 nm. Commercial providers have a standard set of filters, but users may select optional filters when required. A complex of four or eight digital cameras with different filters allow multispectral data to be collected (Anderson and Yang 1996; Everitt et al. 1986, 1987; King 1995; Louis et al. 1995; Manzer and Cooper 1982; Sun et al. 1997). Many government agencies (United States Department of Agriculture—Agricultural Research Service, United States Forest Service, and United States Bureau of Land Management) and universities (University of Minnesota, Simon Fraser University, University of Idaho, Mississippi State University, Purdue, Utah State University, and many more) own this type of sensor system. Positive Systems Inc. and Red Hen Systems Inc. were early commercial developers of video multispectral systems that were used to map weeds in rangeland, pastures, and forest. Costs for image acquisition from commercial companies range from $17,000 to $35,000 for a 20- by 40-km image area for a 1-m spatial resolution data set with four spectral bands.[9] Airborne multispectral digital imaging systems are commonly used to map woody and herbaceous weeds on rangelands and forest (Carson et al. 1995; Everitt and Nixon 1985; Everitt et al. 1991, 1992; Lass and Callihan 1997; Lass et al. 1996).

Reducing the spatial resolution to 0.5 or 1 m does not always ensure that weed infestations in rangeland, pasture, or forest environments will be detectable. Weeds may have similar spectral reflectance to other vegetation or may be mixed in other vegetation (Shafii et al. 2004). Hyperspectral sensors are imaging spectrometers that sample the reflected solar region of the electromagnetic spectrum in narrow, continuous increments. The continuous increments allow for blue, green, red, and near-infrared spectra to be recorded instead of a single value. One hyperspectral sensor is the NASA Jet Propulsion Laboratory Airborne Visible/Infrared Imaging Spectrometer (AVIRIS).[10] The AVIRIS sensor is a 224-band system measuring light between 400 and 2,500 nm with 10-nm increments. The spatial resolution for high-altitude AVIRIS is 20 by 20 m with a swath width of 11 km when mounted in a NASA ER-2 (modified U2) aircraft, and low-altitude AVIRIS is 4 by 4 m with a swath width of 4 km when mounted in a Twin Otter aircraft. Several invasive weed species have been detected with the AVIRIS sensor (DiPietro 2002; Parker-Williams and Hunt 2002, 2004; Underwood et al. 2003; Ustin et al. 2002). The high demand for hyperspectral data for mineral and oil exploration needs have allowed commercial companies to enter this market. Two pioneering hyperspectral companies are Earth Search Sciences (ESSI) and Innovation Technology Research Excellence Service (ITRES). The Probe hyperspectral sensors of ESSI have 128 bands with a spectral resolution between 450 and 2,500 nm ranging from 12- to 16-nm bandwidth. The spatial resolution can be 3 to 4 m depending on the height of the aircraft. The CASI system of ITRES has a spectral resolution between 400 to 1,000 nm and the bandwidth is 12 nm. The spatial resolution ranges from 0.5 to 10 m depending on the height of the aircraft. The CASI system is fully programmable to record only the desired spectral bands. New upgrades to the CASI system have increased the spectral range to 2,500 nm and added thermal detection (8,000 to 12,000 nm). The typical cost for hyperspectral data from a commercial company varies between $60,000 and $100,000 for a 20- by 40-km area and 2- to 3-m spatial resolution.[11] This amount may be as low as $6,000 for a 20- by 2-km area with 3-m spatial resolution when obtained for research mode with multiple researchers sharing the mobilization costs. Several other companies have started to market hyperspectral sensors, so data acquisition costs are expected to decrease. Hyperspectral sensors have been used to detect Brazilian pepper (Lass and Prather 2004), spotted knapweed (Lass et al. 2002), yellow starthistle (*Centaurea solstitialis* L.) (Lass and Thill 2000), and aquatic vegetation (Bostater et al. 2004).

New hybrid multispectral–hyperspectral sensors offer the best of both airborne sensors. Flight Landata Inc.[12] has a dual-use system with both hyperspectral and multispectral airborne data acquisition capabilities. The High Definition Hyperspectral Imaging System is a hyperspectral and multispectral image data acquisition system using a light aircraft platform. The system integrates a hyperspectral imager (HSI)–multispectral imager (MSI), an inertial navigation system (INS), and a data acquisition computer. The HSI is a grating imaging spectrometer using a 1.6 cm charged-coupled device (CCD) digital camera that has a 16-mm focal length lens. The sensor splits the visible and infrared light spectrum (445 to 900 nm) into 240 bands with a spectral resolution better than 2.5 nm. The MSI has four megapixel CCD cameras with interchangeable filters that acquire data in four bands at user-selected wavelengths. The MSI footprint is a 1,280 × 1,030 CCD array of progressively scanned images formatted with eight-bit quantization (image data compression algorithm). Currently, four 10-nm bandwidth interference filters with center pass wavelengths of 450, 550, 650, and 800 nm are mounted on the 16-mm focal length lenses. The INS integrates two positioning components: a differential GPS to locate the plane and three precision gyroscopes that comprise the inertial measurement unit to track plane tilt (pitch, roll, and yaw). Images are acquired and georeferenced without the need of ground control point acquisition. These hybrid sensors are currently being tested for detection of invasive weeds, and preliminary results appear to be promising.

Processing Algorithms

The complex nature and the amount of digital data collected with modern sensors requires the use of computer software[13] and algorithms to group pixels into classes before observing on the screen (Campbell 2002). Image classification falls into two general methods referred to as supervised and unsupervised. In supervised classification, known spectral reflectance values either derived from known locations on the image or handheld spectrometers are used to identify other pixels having the same reflection. In unsupervised classification, the computer groups all reflections having the same pattern, and the groups are identified from known weed infestations on the ground (Campbell 2002).

Algorithms used for supervised classifications are either distance based (hard classifiers) or unmixing based (soft classifiers) (Campbell 2002). Hard classifiers use the distance from a known reflectance value to determine if the value matches an unknown pixel. Spectral angle mapper (SAM) (Kruse 1993), maximum likelihood (MLH), and minimum distance to mean (MDM) algorithms are often used as a "first look" tool to identify whether the weed is present or absent (Campbell 2002). SAM, MLH, and MDM assume that the reference values (training data) are pure and represent 100% cover of the feature (plant population) (Campbell 2002; Carson et al. 1995; Lass et al. 2002).

SAM quantifies the classification separability based on the angle between two vectors that point to the center of the known target reflectance value and the pixel value (Kruse et al. 1993). A narrow angle will produce classified images with the highest likelihood of matching a pure population. Increasing the classification angle will increase the number of pixels being classified, whereas decreasing the classification angle reduces the number of pixels classified. As the angle widens, the classification includes deviations from the pure reflectance that contain a mix of the target and spectral background. The widening angle also includes features that may have similar reflectance to the target weed, increasing the commission error (identified on the image but not on the ground). The SAM algorithm is insensitive to changes in brightness because the vector angle is used and not the vector length (Campbell 2002; Kruse et al. 1993).

The MLH and MDM algorithms use the mean reflectance of each band to define the spectral reflectance pattern for a species (Campbell 2002). Unknown pixels of the image are assigned to the class with the closest matching value. The maximum distance from the mean threshold may be set to reduce the overcommitment classification error. MLH and MDM are sensitive to changes in brightness, and images within the study site should be concatenated together before classification (Carson et al. 1995).

The SAM and MDM classifications result in images displaying the best match to known spectra for each pixel. Overlaying classified images with widening angles or distance thresholds produces maps describing a range of detection likelihoods from high to low as the pure reflectance value is diluted with mixed vegetation (Lass and Prather 2004).

Soft classification algorithms such as linear spectral unmixing (LSU), mixture-tuned matched filtering (MTMF), and Bayesian Probability have been used to detect leafy spurge (Parker-Williams and Hunt 2002, 2004) and yellow starthistle (Shafii et al. 2004). To work properly, soft classification algorithms need to have a spectral reflectance pattern for all existing vegetation features and weed groups. Spectral reflectance patterns from the known weed locations on the images or handheld spectrometer readings are used for classifying each pixel. The output is not a single classified vegetation map but a set of images (one per vegetation feature) that expresses, for each pixel, an estimate of occurrence in each class. These algorithms are valuable tools for monitoring changes in established weed populations due to environmental conditions and control activities.

The LSU algorithm assumes that a pixel value is a linear combination of all spectral components present in the pixel and that all features on the image are represented in the pixel in some proportion (Campbell 2002). For example, a pixel containing only a single weed should have the same value as reflected in a weed patch with 100% cover. If the weed cover is only 50% and the remaining is grass, then the pixel value should be the mean of the reflectance values for the weed and grass. The LSU algorithm is most effective when there are a few distinct cover types. LSU may not be practical for most weed detection projects because the reflectance patterns for all the cover types are seldom measured. In these cases, MTMF may be used as an alternative. MTMF is a "partial" unmixing algorithm (Boardman et al. 1995) that produces two images representing percent target abundance and a measure of feasibility without prior knowledge of the spectral characteristics of background features (e.g., under story vegetation and soil). It has been effective in reducing classification error when detecting leafy spurge (Parker-Williams and Hunt 2002, 2004).

The Bayesian probability algorithm estimates the probability that a pixel value belongs to the weed class or other feature classes based on prior knowledge of the statistical distribution of the feature (Shafii et al. 2004). Prior knowledge may include knowledge of the spatial distribution. The prior knowledge is used to estimate the probability that the unknown pixel has membership in a feature class. A Bayesian probability algorithm can reduce classification error.

Algorithms used for unsupervised classifications are either frequency based or artificial signature based. Frequency-based algorithms use a histogram peak technique to define classification groups (Richards 1986). A classification group is a peak where the frequency is higher than all of its neighbors. Once the group is defined, pixels are assigned to the nearest peak based on the number of desired classes defined by the user. Once the image has been grouped into classes, the known locations in the field are used to identify each class. This method of classification has successfully classified multispectral images where weed cover is more than 50% (Carson et al. 1995; Lass et al. 1996).

Artificial signature development algorithms use posteriori least square orthogonal subspace (PLOS) projections to develop spectral reflectance files for the image or selected sites within the image (Chang 1999; Chang and Ren 2000; Chang et al. 1998; Ren and Chang 1998). The LSU logic of PLOS algorithm selects the maximum spectral values for the image across all bands based on the sum of squares to calculate the first spectral reflectance curve. The next spectral reflectance curve is identified by finding those values dissimilar to the first set of values for all bands. The algorithm repeats this process until the user-defined number of spectral reflectance curves has been developed (Settle and Drake 1993; Shimabukuro and Smith 1991; Sohn and McCoy 1997). Images are then classified with a hard classifying algorithm (Lass and Prather 2004). Artificial signature development algorithms are ideal for calculating spectral signatures when spectral reflectance files collected from a handheld spectrometer and image data does not work because of mixed vegetation on the ground (Lass and Prather 2004).

There are several other algorithms commonly used to help detect weeds in rangeland and pastures. The use of vegetation and stress indices offers the opportunity to identify locations where weeds can expand or become established. These indices ratio red and near-infrared or red and mid-infrared bands to estimate the percent green vegetation cover or healthy vegetation (Anderson et al. 1993; O'Neill 1996). Vegetation indices are very useful for detecting invasive plants when the weed senesces before native vegetation. The normalized difference vegetation index is the most recognized vegetation index and has been successfully used to predict potential distribution of Dyers woad (*Isatis tinctoria* L.) (Dewey and Price 1991) and detect downy brome (*Bromus tectorum* L.) in rangeland (USGS 2003).

A Case Study: Detecting Spotted Knapweed and Babysbreath with Hyperspectral Data

The review of the literature only lays the foundation to allow research to build on. We offer this working example as advancement in hyperspectral remote sensing research. Spotted knapweed is widely distributed in Idaho, and babysbreath is found in a few locations in Idaho. In the western United States, both species have been observed to invade sagebrush (*Artemisia* spp.) communities (Roche and Talbott Roche 1994). Babysbreath thrives in moisture levels from 25 to 100 cm annually and prefers sandy soil (Darant 1975; Darant and Coupland 1966). In general, spotted knapweed plants prefer moister conditions than babysbreath does. Although babysbreath is on many invasive species lists, and California and Washington's noxious weed list, it is aggressively harvested by the cut flower industry. The wild babysbreath plants are prized for their short stems and multiple branches (Schlosser et al. 1991).

Image acquisition timing is critical to species-level discrimination. Detection of spotted knapweed and babysbreath requires associated annual grasses and their understory vegetation to be fully matured and bleached yellow or a distinctly different color (Lass et al. 2002). In this study, babysbreath was imaged before flowering, but the flower stalks were present and plants had reached their maximum size. A babysbreath plant has multiple branched stems growing to 1 m height that form a bunch about as wide as it is tall. The detection of spotted knapweed is dependent on some residual stems being present from previous year's growth, and background vegetation is not dominating the reflectance (Lass et al. 2002).

A previous study showed that spotted knapweed infestations dominating a landscape are detectable with hyperspectral sensors (Lass et al. 2002). The previous study used two locations where the populations had been present for more than 30 yr and filled most of the suitable habitats. The previous study used a "whiskbroom style" imaging spectrometer that sampled the reflected solar region of the electromagnetic spectrum ranging from 440 to 2,543 nm with 12- to 16-nm bandwidths and a spatial resolution of 5 m. Results demonstrated that spotted knapweed was detectable using a SAM classification when cover densities were greater than 70% and populations were larger than 0.1 ha.

The objectives of this study were (1) to determine if a "CCD push-broom style" (415 and 953 nm with 11- to 12-nm [± 6-nm] bandwidth) could detect spotted knapweed and babysbreath and (2) to determine if sparse patches (10 to 20% weed cover) of spotted knapweed and babysbreath were detectable.

Materials and Methods

This study used hyperspectral images of the Swan Valley in Idaho acquired on July 27, 2002, and July 7, 2003. Spotted knapweed and babysbreath start to flower from mid to late July in the Swan Valley. For both weeds, images collected in 2002 were during flower production, but images collected in 2003 were before flowering. The bounding coordinates for the 2002 flight area were latitude 43°22′12.5″ and 43°29′21.1″N and longitude 111°15′42.9″ and 111°20′08.8″W. The bounding coordinates for the 2003 flight area were latitude 43°22′12.5″ and 43°29′21.1″N and longitude 111°15′42.8″ and 111°20′10.0″W. Overlap between 2002 and 2003 images was sufficient to allow all babysbreath validation sites to be used in both years. Images collected in 2002 showed 22 spotted knapweed validation sites and 2003 images showed all 28 spotted knapweed validation sites. Not all other vegetation sites could be used in the first year.

The instrument used was a CCD sensor collecting data along the flight line.[14] Spectral reflectance was measured between 415 and 953 nm with 12-nm increments to make a 48-band data set. The spatial resolution was 2 m. The data provider rectified the images to ground coordinates. In 2002, the data provider atmospherically corrected the images and the images were ready to classify. In 2003, the data were acquired without atmospheric correction and required atmospheric correction (Chavez 1996; Forster 1984) before classification.

Spectral reflectance curves were developed from image-based spectral files using sites on the ground with 70 to 100% spotted knapweed or babysbreath cover and 0 to 30% mature downy brome grass cover (Lass et al. 2002). Selection of pixels to be used within the sites was based on the darkness of the pixel when band 10 (573 nm) was displayed on the monitor (darker pixels were assumed to be pure weed cover because the background vegetation was mature annual brome). The spectral training development site for spotted knapweed contained 23 to 38 pixels at three locations, and babysbreath had 20 pixels at two locations. Spectral reflectance curves developed from the 2002 images were used to classify both the 2002 and 2003 data. Images were classified using the SAM algorithm in Idrisi[15] (Kruse et al. 1993). SAM angles selected for testing were based on estimated overall image classification error when compared with ground truth data. The classification angles used were 1, 2, 3, 4, 5, and 10°.

Validation data were collected outside the spectral reflectance development sites. GPS receivers with Wide Area Augmentation System (WAAS) were used to record 28 polygons containing spotted knapweed, 4 polygons with both spotted knapweed and babysbreath, and 11 polygons containing babysbreath. GPS accuracy was between 1 and 2 m based on comparing recorded positions of weed and other features with a U.S. Geological Survey Digital Orthophoto Quarter Quad image. These polygons represented 84,734 pixels with spotted knapweed and 71,986 pixels of babysbreath, respectively. Spotted knapweed cover at most sites was 20 to 60% but ranged from 1 to 100% (only 7 of the 32 polygons had greater than 50% spotted knapweed cover). The babysbreath cover in the verification sites ranged from 30 to 100%. Other vegetation features included 23,093 pixels in alfalfa (*Medicago sativa* L.), 78,570 pixels in aspen (*Populus tremuloides* Michx.), 2,067 pixels in Canada thistle [*Cirsium arvense* (L.) Scop.]/grasslands, 18,503 pixels in grassland, 4,038 pixels of leafy spurge, 22,995 pixels of juniper (*Juniperus* spp. L.)/pine (*Pinus ponderosa* P. & C. Lawson)/sagebrush (*Artemisia* L.)/shrub/grass, 13,054 pixels of annual grass, and 3,923 pixels of wheatgrass [*Agropyron cristatum* (L.) Gaetn.]. Locations of the verification sites were delimited as vector data and converted to raster images with the same spatial resolution as the classified images to allow cross tabulation with the image data in an error matrix for both the 2002 and 2003 classification assessment.

Mixed reflectance values within a pixel from associated vegetation produced high omissional errors when classified with narrow spectral angles. Classification of hyperspectral data typically uses an unmixing algorithm like LSU or MTMF to estimate the relative fraction of each element to solve the high omissional error problem from 1 to 2° classification angles (Parker-Williams and Hunt 2002).

A spatial technique was used to reduce detection errors. The seed morphology for spotted knapweed and babysbreath suggests that most seeds are scattered within a few meters of the parent plant (Roche and Talbott Roche 1994). Pixels classified using SAM with a narrow spectral angle were buffered to 500 m (Lass and Prather 2004), and then a second SAM classification with a wider angle was performed. Pixels classified within the original 500-m buffer were considered to have a higher probability of containing spotted knapweed or babysbreath than those outside the

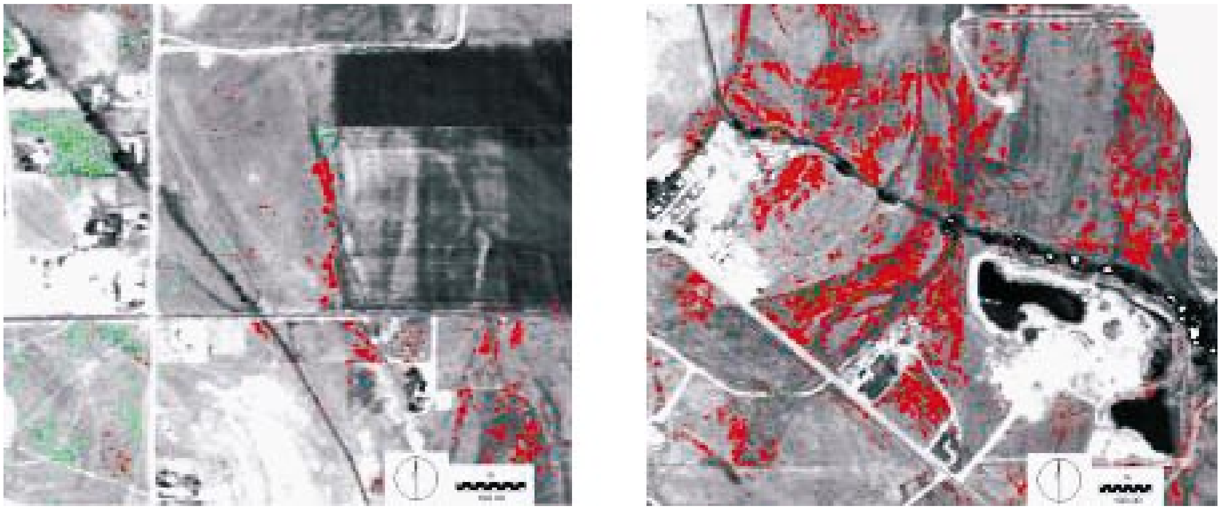

FIGURE 1. Hyperspectral images showing spotted knapweed in red and babysbreath in green.

buffer. The 500-m buffer area was selected on the basis of a previous study (Lass et al. 2002) and because it is easily searchable by ground crews. The buffered images were then used to isolate pixels in the image classified with low omissional error and high commissional error (Lass and Prather 2004).

An error matrix was created to determine image classification accuracy of both the 2002 and 2003 images by contrasting the classified image with ground validation data (Card 1982; Congalton 1991; Congalton et al. 1983; Goodchild and Gopal 1989). Omissional (present on the ground but not on the image) and commissional error (present on the image but not on the ground) rates were calculated from the differences between ground truth and classified images in the matrix (Congalton et al. 1983; Lass and Prather 2004; Lass et al. 2000, 2002). Errors in delineating sparse infestations and positional errors for small infestations made assessing individual pixel classification accuracies impossible. Errors of omission were estimated by counting the number of validation sites positioned and recorded as polygon data with the GPS being detected by the classified images. Errors of commission were estimated by counting the number of false-positive spotted knapweed and babysbreath on the images when compared with validation data and calculating commissional error based on an error matrix for the nonweed classes.

Results and Discussion

Spotted knapweed and babysbreath infestations were detectable in both the 2002 and 2003 hyperspectral images. Figure 1a shows a spotted knapweed infestation in red from the 2003 images when classified with a 2° angle. Figure 1b shows a babysbreath infestation in green and spotted knapweed infestation in red from the 2003 images when classified with a 2° angle.

The 2003 classified images detected spotted knapweed at 21 of 28 sites containing 10 to 100% cover spotted knapweed on the ground when the classification angle was set to 5° (Table 1). Sites where spotted knapweed infestations were on the ground, but not classified in the images, were typically located in irrigated pastures or near canals with higher moisture. The processed imagery also showed spotted knapweed in 9 of 15 babysbreath verification sites with cover ranging from 20 to 100% when the classification angle was set to 5°. Images incorrectly identified 3 of 32 sites of spotted knapweed–free sites as spotted knapweed on the ground when the classification angle was 3° or wider. Two of these false detections were alfalfa–grass fields used for hay and one site was grassland infested with leafy spurge. The images did not show other alfalfa–grass hayfields or leafy spurge–infested sites as infested with spotted knapweed.

Images classified for spotted knapweed detected 15 of 22 validation sites in 2002 at 5° (Table 1). Five of the seven sites on the images not indicating spotted knapweed were in irrigated pastures or in moist areas adjacent to a canal and grazed. One undetected spotted knapweed site had less than 25% weed cover, although other sites with similar weed cover were detected. The size of this verification site was three pixels, and some image georectification error may have contributed to the misclassification. The lack of detection of the known spotted knapweed within the babysbreath population may have been due to environmental conditions of the later flight date in 2002.

Overall average spotted knapweed site detection rates for the 2 yr was 67% for cover classes ranging from 1 to 100% when classified with SAM using a 5° angle (Table 2). Irrigated pastures had high errors of omission, and if properly classified, the overall spotted knapweed detection rate would have been 86% of the validation sites on the ground. SAM classification did not define the extent of invasion in a site because of low uneven knapweed cover found within a weed patch in dry growing conditions. The previous study detecting spotted knapweed was located in an area where plants were robust, moisture was adequate and the plants were not grazed (Lass et al. 2002). Significant results of this study show that spotted knapweed infestations are detectable in semiarid rangelands with a hyperspectral sensor measuring light in the visible and near-infrared range.

The 2003 images classified for babysbreath showed 14 of 15 verification sites located on the ground when a 3° classification angle was used. The one site not represented on the babysbreath images was a small strip of babysbreath (30 to 60% cover) about 6 by 12 m in size with 20% sagebrush

Table 1. Spotted knapweed and babysbreath site detections with a hyperspectral image.

	Classification angle used with spectral angle mapper algorithm											
2003 Images	1		2		3		4		5		10	
Classification	On image		On image		On image		On image		On image		On image	
On ground	Spotted knapweed	Other veg.	Spotted knapweed	Other veg.	Spotted knapweed	Other veg.	Spotted knapweed	Other veg.	Spotted knapweed	Other veg.	Spotted knapweed	Other veg.
	no. of sites											
Spotted knapweed	4	25	16	12	17	11	20	8	21	7	23	5
Spotted knapweed mixed with babysbreath	4	11	7	8	7	8	9	6	9	6	9	6
Other vegetation	0	33	1	32	3	29	3	29	3	29	3	29
Babysbreath classification	On image		On image		On image		On image		On image		On image	
On ground	Babys-breath	Other veg.	Babys-breath	Other veg.	Babys-breath	Other veg.	Babys-breath	Other veg.	Babys-breath	Other veg.	Babys-breath	Other veg.
	no. of sites											
Babysbreath	6	9	12	3	14	1	14	1	14	1	14	1
Other vegetation	0	62	4	58	8	54	9	53	10	52	11	51
2002 Images												
Spotted knapweed classification	On image		On image		On image		On image		On image		On image	
On ground	Spotted knapweed	Other veg.	Spotted knapweed	Other veg.	Spotted knapweed	Other veg.	Spotted knapweed	Other veg.	Spotted knapweed	Other veg.	Spotted knapweed	Other veg.
	no. of sites											
Spotted knapweed	9	13	11	11	13	9	14	8	15	7	15	7
Spotted knapweed mixed with babysbreath	0	15	0	15	0	15	0	15	0	15	0	15
Other vegetation	0	6	0	6	1	5	1	5	1	5	1	5
Babysbreath classification	On image		On image		On image		On image		On image		On image	
On ground	Babys-breath	Other veg.	Babys-breath	Other veg.	Babys-breath	Other veg.	Babys-breath	Other veg.	Babys-breath	Other veg.	Babys-breath	Other veg.
	no. of sites											
Babysbreath	11	4	14	1	14	1	15	0	15	0	15	0
Other vegetation	3	26	9	20	10	19	10	19	10	19	11	18

Table 2. Omissional and commissional error rates when classifying spotted knapweed and babysbreath cover using six classification angles.

	Classification angle used with spectral angle mapper algorithm					
	1	2	3	4	5	10
	%					
Commissional error						
Spotted knapweed	0.0 ± 0.0[a]	2.8 ± 2.1	9.8 ± 5.9	8.5 ± 5.0	8.1 ± 4.8	7.8 ± 4.6
Other	62.1 ± 9.6	54.8 ± 10.7	55.8 ± 11.1	52.1 ± 11.4	50.7 ± 11.5	49.2 ± 11.6
Omissional error						
Spotted knapweed	79.0 ± 10.1	57.5 ± 10.9	53.8 ± 10.9	46.2 ± 10.5	43.7 ± 10.3	41.2 ± 10.1
Other	0.0 ± 0.0	2.6 ± 2.0	10.6 ± 6.3	10.5 ± 6.2	10.5 ± 6.2	10.5 ± 6.2
Overall error	53.3 ± 8.9	39.5 ± 8.4	39.8 ± 8.4	34.7 ± 8.0	33.0 ± 7.8	31.3 ± 7.7
Commissional error						
Babysbreath	15.0 ± 9.5	33.3 ± 12.7	39.1 ± 12.7	39.5 ± 12.5	40.8 ± 13.0	43.1 ± 12.6
Other	12.9 ± 5.2	4.9 ± 2.9	2.7 ± 1.9	1.3 ± 1.0	1.4 ± 1.3	1.4 ± 1.1
Omissional error						
Babysbreath	43.3 ± 16.0	13.3 ± 7.9	6.6 ± 4.6	3.3 ± 2.6	3.3 ± 3.3	3.3 ± 2.6
Other	3.3 ± 2.1	14.3 ± 5.7	19.8 ± 6.9	20.9 ± 7.1	21.9 ± 7.2	24.1 ± 7.6
Overall error	13.2 ± 4.9	14.0 ± 5.0	16.5 ± 5.5	16.5 ± 5.5	17.4 ± 5.8	19.0 ± 6.0

[a] Bayesian 95% lower and upper probability bounds.

cover. Plants at this site appeared to be slightly smaller that other babysbreath plants in the area. Other babysbreath sites with sagebrush were classified correctly. The 2003 images misclassified four validation sites as babysbreath when a 2°-classification angle was used out of 62 verification sites. Three of these sites contained meadow brome (*Bromus erectus* L.) and spotted knapweed, whereas one of the sites just had meadow brome. This would suggest some overlay of spectral reflectance values for spotted knapweed and meadow brome. Increasing the classification angle to 3° increased the number of false detections to eight.

The 2002 image classified for babysbreath showed that all validation sites having babysbreath were detected by the hyperspectral data when a 4°-classification angle was used. One site was not detected at 2- and 3°-classification angles, and the 1°-classification angle identified 11 of the 15 validations sites (Table 1). The 1°-classification angle overcommitted and found 3 of 29 sites indicating the false presence of babysbreath on the ground. These misclassified sites were a grass pasture infested with spotted knapweed, grass area infested with Canada thistle, and an alfalfa grass hayfield. The misclassification probably was a result of hay harvest and possible uneven regrowth, but this speculation is based on visual observation made in 2003.

The 2-yr site detection rate for babysbreath was 83.5% (overall accuracy) for cover classes ranging from 30 to 100% when classified with SAM using a 4° angle (Table 2). The stems arranged in a small tight bunch made babysbreath easy to detect with high-resolution hyperspectral data when compared with the scattered plants found when many species invade a site.

Early detection of invasive species maximizes the potential for long-term control and minimizes the impact to the environment. In our study, spotted knapweed and babysbreath were detected with hyperspectral data, although the extent of the infestation within a population was not delineated. Ground survey crews will need to define the extent of the population; however, the results of this study indicate that SAM-processed hyperspectral imagery can provide guidance to field crews on where to start their surveys.

Detection of many weeds invading rangeland, pastures, and forest with remote sensing is possible with current technology, but applications are often repeated demonstrations on the same species and the same or different locations. How many times do we need to image an invasive weed in a demonstration area before the weed has spread to become a countywide or statewide project? Improved automated preprocessing of the images is necessary for this technology to expand market share against traditional survey techniques. Images need to be classification ready with accurate atmospheric and radiometric correction and rectified to ground coordinates. Most land managers will not tolerate positional error when the GPS and GIS data do not match the weed location from the remote sensing image. Integrating remote sensing data into a GIS for postprocessing and ultimate transfer of the data to handheld computers allows field crews to use the data to focus and monitor treatments. Trained personnel will be required to use, update, and maintain data. Students in geographic science need a better understanding of weed science much like students in weed science need a better understanding of geographic science. The technology of remote sensing of invasive weeds in rangelands, pastures, and forests has moved forward, and the challenge is making the data usable to locate weeds on the ground in an operational context.

Sources of Materials

[1] NASA Landsat MSS, U.S. Geological Survey, EROS Data Center, 47914 252nd Street, Sioux Falls, SD 57198 (multispectral satellite images).

[2] Prices for raw data included for informational purposes; actual cost may be more for value-added processing to rectify images to ground coordinates and correct for sensor and atmospheric attenuations.

[3] NASA Thematic Mapper TM, U.S. Geological Survey, EROS Data Center, 47914 252nd Street, Sioux Falls, SD 57198 (multispectral satellite images).

[4] NASA Enhanced Thematic Mapper ETM+ U.S. Geological Survey, EROS Data Center, 47914 252nd Street, Sioux Falls, SD 57198 (multispectral satellite images).

[5] NASA Earth Observing Satellite EO-1, U.S. Geological Survey, EROS Data Center, 47914 252nd Street, Sioux Falls, SD 57198 (multispectral and hyperspectral satellite images).

[6] NASA Advanced Very High Resolution Radiometer AVHRR, U.S. Geological Survey, EROS Data Center, 47914 252nd Street, Sioux Falls, SD 57198 (free multispectral satellite images).

[7] Spot Image Corp., 14595 Avion Parkway, Suite 500, Chantilly, VA 20151 (high spatial resolution multispectral satellite images).

[8] Ikonos data, Space Imaging Inc., 12076 Grant Street, Thornton, CO 80241, and Quickbird, Digital Globe, 1601 Dry Creek Drive, Suite 260, Longmont, CO 80503. Cost of image acquisition based on phone quote made in August 2004 (high spatial resolution multispectral satellite images).

[9] Positive Systems Inc., 713 East 13th Street, Whitefish, MT 59937, and Red Hen Systems Inc., 2850 McClelland, Suite 3900, Fort Collins, CO 80525 (digital video and multispectral cameras).

[10] Airborne Visible/Infrared Imaging Spectrometer (AVIRIS), Jet Propulsion Laboratory, M/S 171-B1, 4800 Oak Grove Dr., Pasadena, CA 91109 (high spatial resolution hyperspectral images).

[11] Earth Search Sciences (ESSI), 1729 Montana Highway 35, Kalispell, MT 59901, and Innovation Technology Research Excellence Service (ITRES) 400 Inverness Drive South, Suite 330, Englewood, CO 80112 (high spatial resolution hyperspectral images).

[12] Flight Landata Inc., One Parker Street, Lawrence, MA 01843 (high spatial resolution hyperspectral sensors).

[13] A partial list of software for image processing includes ERDAS from Leica Geosystems GIS and Mapping LLC, ERDAS, 2801 Buford Highway, N.E. Atlanta, GA 30329; Hypercube, U.S. Army Corps of Engineers, Topographic Engineering Center, 7701 Telegraph Road, Alexandria, VA 22315; Idrisi Kilimanjaro from Clark University, 950 Main Street, Worcester, MA 01610; ENVI from Research System Inc., 4990 Pearl East Circle, Boulder, CO 80301; a good online tutorial is the NASA Tutorial, NASA/Goddard Space Flight Center, Code 420, Greenbelt, MD 20771.

[14] The hyperspectral sensor was a CASI 2005 built and owned by ITRES, Inc., 400 Inverness Drive South, Suite 330, Englewood, CO 80112-5830 and subcontracted through Aquilavision, 1121 East Broadway, Suite 105, Missoula, MT 59802.

[15] Idrisi Kilimanjaro v14.2 Clark Labs, Clark University, 950 Main Street, Worcester, MA 01610.

Acknowledgments

The authors are grateful to the Bonneville County weed survey crew and Mark Strom of Boise State University for their work in delimiting spotted knapweed and babysbreath. Portions of this research were funded through the competitive award of the 2001 NASA Earth Science Enterprise Broad Agency Announcement for State, Local, and Tribal Uses of Remote Sensing and Geospatial Information implemented out of the John C. Stennis Space Center in Mississippi.

Literature Cited

Anderson, G. L., J. H. Everitt, D. E. Escobar, N. R. Spencer, and R. J. Andrascik. 1996. Mapping leafy spurge (*Euphorbia esula*) infestations using aerial photography and geographic information systems. Geocarto Int. 11:81–89.

Anderson, G. L., J. H. Everitt, A. J. Richardson, and D. E. Escobar. 1993. Using satellite data to map false broomweed (*Ericameria austrotexana*) infestations on south Texas rangelands. Weed Technol. 7:865–871.

Anderson, G. L., J. D. Hanson, and G. F. Hart. 1992. Developing Relationships Between Green Biomass and Landsat Thematic Mapper Derived Vegetation Indices on Semi-Arid Rangelands. Washington, DC: ASPRS/ACSM/RT 92. Volume 4. Pp. 355–363.

Anderson, G. L. and C. Yang. 1996. Multispectral videography and geographic information systems for site-specific farm management. Pages 681–692 *in* Proceedings of the 3rd International Conference on Precision Agriculture. Madison, WI: ASA/CSSA/SSSA.

Arnold, G. W., P. G. Ozanne, K. A. Galbraith, and F. Dandridge. 1985. The capeweed content of pastures in south-west Western Australia. Aust. J. Exp. Agric. 25:117–123.

Bellmund, S. and W. Kitchens. 1997. Landscape Ecological Indices in Ecological and Precursor Success Criteria for South Florida Ecosystem Restoration. www.fiu.edu/~glades/taskforce/precursor/chapter7.html.

Boardman, J. W., F. A. Kruse, and R. O. Green. 1995. Mapping target signature via partial unmixing of AVIRIS data. Pages 23–26 *in* Summaries of the Fifth JPL Airborne Geoscience Workshop JPL Publication 95-1. Pasadena, CA: NSAS Jet Propulsion Laboratory.

Bostater, C. R., T. Ghir, L. Bassetti, C. Hall, E. Reyeier, R. Lowers, K. Holloway-Adkins, and R. Virnstein. 2004. Hyperspectral remote sensing protocol development for submerged aquatic vegetation in shallow waters. Proc. SPIE Int. Soc. Opt. Eng. 5233:199–215.

Campbell, J. B. 2002. Introduction to Remote Sensing. 3rd ed. New York: Gulford. 622 p.

Card, D. H. 1982. Using known map category marginal frequencies to improve estimates of thematic map accuracy. Photogram. Eng. Remote Sens. 48:431–439.

Carson, H. W., L. W. Lass, and R. H. Callihan. 1995. Detection of yellow hawkweed with high resolution digital images. Weed Technol. 9:477–483.

Chang, C. I. 1999. Least squares error theory for linear mixing problems with mixed pixel classification for hyperspectral imagery. Recent Res. Dev. Opt. Eng. 2:214–268.

Chang, C. I. and H. Ren. 2000. An experiment-based quantitative and comparative analysis of target detection and image classification algorithms for hyperspectral imagery. IEEE Trans. Geosci. Remote Sens. 38:1044–1063.

Chang, C. I., X. Zhao, M.L.G. Althouse, and J. J. Pan. 1998. A posteriori least squares orthogonal subspace projection approach to mixed pixel classification in hyperspectral images. IEEE Trans. Geosci. Remote Sens. 36:898–912.

Chavez, P. S. 1996. Image-based atmospheric corrections—revisited and improved. Photogram. Eng. Remote Sens. 62:1025–1036.

Congalton, R. G. 1991. A review of assessing the accuracy of classifications of remotely sensed data. Remote Sens. Environ. 37:35–46.

Congalton, R. G., R. Oderwald, and R. A. Mead. 1983. Assessing Landsat classification accuracy using discrete multivariate analysis statistical techniques. Photogram. Eng. Remote Sens. 49:1671–1678.

Darant, A. L. 1975. The biology of Canadian weeds. *Gypsophila paniculata* L. Can. J. Plant Sci. 55:1049–1058.

Darant, A. L. and R. T. Coupland. 1966. Life history of *Gypsophila paniculata*. Weeds 14:313–318.

Dewey, S. A. and K. P. Price. 1991. Satellite remote sensing to predict potential distribution of dyers woad (*Isatis tinctora*). Weed Technol. 5: 479–484.

DiPietro, D. Y. 2002. Mapping the Invasive Plant *Arundo donax* and Associated Riparian Vegetation Using Hyperspectral Remote Sensing. www.great.jussieu.fr/great/theses/master_Dipietro_2002.pdf

Everitt, J. H., M. A. Alaniz, and D. E. Escobar. 1992. Using remote sensing to distinguish common goldenweed (*Isocoma coronopifolia*) and Drummon goldenweed (*Isocoma drummondii*). Weed Sci. 40:621–628.

Everitt, J. H. and C. J. Deloach. 1990. Remote sensing of Chinese Tamarisk (*Tamarix chinensis*) and associated vegetation. Weed Sci. 38:273–278.

Everitt, J. H., D. E. Escobar, M. A. Alaniz, and M. R. Davis. 1987. Using airborne middle-infrared (1.45–2.0 μm) video imagery for distinguishing plant species and soil conditions. Remote Sens. Environ. 22: 423–428.

Everitt, J. H., D. E. Escobar, M. A. Alaniz, and M. R. Davis. 1991. Light reflectance characteristics and video remote-sensing of prickly pear. J. Range Manage. 44:587–592.

Everitt, J. H., D. E. Escobar, M. A. Alaniz, M. R. Davis, and J. V. Richerson. 1996. Using spatial information technologies to map Chinese tamarisk (*Tamarix chinensis*) infestations. Weed Sci. 44:194–201.

Everitt, J. H., D. E. Escobar, C. H. Blazquez, M. A. Hussey, and P. R. Nixon. 1986. Evaluation of the mid-infrared (1.45–2.0 μm) with a black-and-white infrared video camera. Photogram. Eng. Remote Sens. 52:1655–1660.

Everitt, J. H. and P. R. Nixon. 1985. Video imagery: a new remote sensing tool for range management. J. Range Manage. 38:421–424.

Forster, B. C. 1984. Derivation of atmospheric correction procedures for LANDSAT MSS with particular reference to urban data. Int. J. Remote Sens. 5:799–817.

Goodchild, M. F. and S. Gopal, eds. 1989. Accuracy of Spatial Databases. London: Taylor and Francis. 309 p.

Haefner, S. 2004. Kite Aerial Photography. www.thehaefners.com/kap/?page=kites.
King, D. J. 1995. Airborne multi-spectral digital camera and video sensors: a critical review of system designs and applications. Can. J. Remote Sens. 21:245–273.
Kruse, F. A., A. B. Lefkoff, J. W. Boardman, K. B. Hiebedrecht, A. T. Shapiro, P. J. Barloom, and A.F.H. Goetz. 1993. The spatial image processing system (SIPS)—interactive visualization and analysis of imaging spectrometer data. Remote Sens. Environ. 44:145–163.
Lass, L. W. and R. H. Callihan. 1997. The effect of phenological stage on detectability of yellow hawkweed (*Hieracium partense*) and oxeye daisy (*Chrysanthemum leucanthemum*) with remote multispectral digital imagery. Weed Technol. 11:248–256.
Lass, L. W., H. W. Carson, and R. H. Callihan. 1996. Detection of yellow starthistle with high resolution multispectral digital images. Weed Technol. 10:466–474.
Lass, L. W. and T. S. Prather. 2004. Detecting the locations of Brazilian pepper trees in the Everglades with a hyperspectral sensor. Weed Technol. 18:437–442.
Lass, L. W., B. Shafii, W. J. Price, and D. C. Thill. 2000. Assessing agreement in multispectral images of yellow starthistle (*Centaurea solstitialis*) with ground truth data using a Bayesian methodology. Weed Technol. 14:539–544.
Lass, L. W. and D. C. Thill. 2000. Detecting yellow starthistle (Centaurea solstitialis) with hyperspectral remote sensing technology. Proc. West. Soc. Weed Sci. 53:11.
Lass, L. W., D. C. Thill, B. Shafii, and T. S. Prather. 2002. Detecting spotted knapweed (*Centaurea maculosa*) with hyperspectral remote sensing technology. Weed Technol. 16:426–432.
Lindholm, S. 2004. Aerial Digital Photography from a Balloon for Fifty Dollars. www.stanford.edu/~lindholm/chpro_bal.html.
Louis, J., D. W. Lamb, G. McKenzie, G. Chapman, A. Edirisinghe, I. McCloud, and J. Pratley. 1995. Operational use and calibration of airborne video for agricultural and environmental land management applications. Pages 326–333 *in* Proceedings of the 15th Biennial Workshop on Colour Photography and Air Videography; Terrahoute, IN. The Regional Institute.
Manzer, F. E. and G. R. Cooper. 1982. Use of portable video taping for aerial infrared imaging of potato disease. Plant Dis. 66:665–667.
O'Neill, A. L. 1996. Satellite-derived vegetation indices applied to semiarid shrublands in Australia. Aust. Geogr. 27:185–199.
Parker-Williams, A. and E. R. Hunt. 2002. Estimation of leafy spurge cover from hyperspectral imagery using mixture tuned matched filtering. Remote Sens. Environ. 82:446–456.
Parker-Williams, A. E. and E. R. Hunt. 2004. Accuracy assessment for detection of leafy spurge with hyperspectral imagery. J. Range Manage. 57:106–112.
Pearlstine, L., S. Smith, E. Walsh, and J. Stenberg. 1998. Aerial Sampling for Brazilian Pepper on Canaveral National Seashore. Gainesville, FL: USGS Biological Resources Division, Florida Cooperative Fish and Wildlife Research Unit.
Peters, A. J., B. C. Reed, and M. D. Eve. 1992. Remote sensing of broom snakeweed (Gutierrezia sarothrae) with NOAA-10 spectral image processing. Weed Technol. 6:1015–1020.
Prather, T. S., B. Shafii, and R. H. Callihan. 1994. Predicting common crupina habitat with geographic and remote sensing data. Pages 122–135 *in* Kansas State University Conference on Applied Statistics in Agriculture. Manhattan, KS: Kansas State University.
Rejmánek, M. and M. J. Pitcairn. 2002. When is eradication of exotic pest plants a realistic goal? Pages 249–253 *in* C. R. Veitch and M. N. Clout, eds. Proceedings of the International Conference on Eradication of Island Invasives. Turning the Tide: The Eradication of Invasive Species. Gland, Switzerland: IUCN SSC Invasive Species Specialist Group.
Ren, H. and C.-I. Chang. 1998. A computer-aided detection and classification method of concealed targets in hyperspectral imagery. Pages 1016–1018 *in* International Symposium Geosciences and Remote Sensing; Seattle, WA. Piscataway, NJ: International Geoscience and Remote Sensing Society.
Richards, J. A. 1986. Remote Sensing Digital Image Analysis: An Introduction. Berlin: Springer. 363 p.
Ringrose, S. and W. Matheson. 1987. Spectral assessment of indicators of range degradation in the Botswana Hardveld Environment. Remote Sens. Environ. 23:379–396.
Roche, B., Jr. and C. Talbott Roche. 1994. Diffuse Knapweed Control in Feral Babysbreath. Washington State Univ. Ext. Bull. 1793. cru.cahe.wsu.edu/CEPublications/eb1793/eb1793.html.
Root, R. 2002. Identification, Canopy, Characterization and Mapping of Invasive Leafy Spurge with the EO-1 Hyperion Orbital Imaging Spectrometer, Final NASA EO-1 Science Validation Team Meeting.
RotorKraft. 2004. RotorKraft: Premium Radio Control Helicopters and Accessories. www.rotorkraft.com/index.htm.
Schlosser, W. E., K. A. Blatner, and R. C. Chapman. 1991. Economic and marketing implications of special forest products harvest in the Costal Pacific Northwest. West. J. Appl. For. 6:67–72.
Settle, J. J. and N. A. Drake. 1993. Linear mixing and the estimation of ground proportions. Int. J. Remote Sens. 14:1159–1177.
Shafii, B., W. J. Price, T. S. Prather, L. W. Lass, and D. C. Thill. 2004. Using landscape characteristics as prior information for bayesian classification of yellow starthistle. Weed Sci. 52:948–953.
Shimabukuro, Y. E. and J. A. Smith. 1991. The least-squares mixing models to generate fraction images derived from remote sensing multispectral data. IEEE Trans. Geosci. Remote Sens. 29:16–20.
Sohn, Y. and R. M. McCoy. 1997. Mapping desert shrub rangeland using spectra unmixing and modeling spectral mixtures with TM data. Photogram. Eng. Remote Sens. 63:707–716.
Sun, X., J. Baker, and R. Hordon. 1997. Computerized airborne multicamera imaging system (CAMIS) and its 4-camera applications. Pages 799–806 *in* Proceedings of the Third International Airborne Remote-Sensing Conference and Exhibition; Copenhagen, Denmark. Ann Arbor, MI: Altarum Airborne Conferences.
Underwood, E., S. L. Ustin, and D. DiPietro. 2003. Mapping nonnative plants using hyperspectral imagery. Remote Sens. Environ. 86:150–161.
[USGS] U.S. Geological Survey. 2003. Monitoring Changes in Vegetation and Land Surfaces by Remote Sensing—Detecting Infestations of Cheatgrass on the Colorado Plateau. climchange.cr.usgs.gov/info/sw/monitor/remote1.html.
Ustin, S. L., D. DiPietro, K. Olmstead, E. Underwood, and G. J. Scheer. 2002. Hyperspectral remote sensing for invasive species detection and mapping. Int. Geosci. Remote Sens. Symp. 3:1658–1660.

Received February 26, 2004, and approved November 22, 2004.